Study on structural and optical properties of TiO_2 ALD coated silicon nanostructures

[1,2]Mykola Pavlenko, [1]Valerii Myndrul, [2]Igor Iatsunskyi[*], [2,3]Stefan Jurga, [1]Valentyn Smyntyna

[1] Department of Experimental Physics, Odessa National I.I. Mechnikov University, 42 Pastera Str., 65023 Odessa, Ukraine
[2] Nanobiomedical Centre, Adam Mickiewicz University, ul. Umultowska 85, PL 61614 Poznań, Poland, yatsunskiy@gmail.com
[3] Department of Macromolecular Physics, Adam Mickiewicz University, 85 Umultowska str., 61-614 Poznan, Poland

ABSTRACT

Structural and optical properties of TiO_2 ALD coated silicon nanostructures were investigated. The morphology and chemical composition of TiO_2 coated silicon nanopillars and porous silicon were studied by using methods of scanning electron microscopy (SEM) and energy dispersive X-ray spectroscopy (EDX). Optical characteristics were studied using measurements of reflectance and luminescence spectra. Detailed analysis of morphological features and photoluminescence mechanisms were provided. Peculiarities of reflectance spectra were discussed. It was shown the possible application of these structures as antireflectance coatings.

Keywords: porous silicon, nanopillars, atomic layer deposition, titanium dioxide.

1. INTRODUCTION

Besides low cost and wide range of application, silicon and silicon-based nanostructures exhibit remarkable optical and electrical properties. Various nanocomposite structures based on porous Si (PSi) are used in different applications such as optics, electronics, catalysis, energy storage, etc [1-4]. The optimization of structural and optical properties of these nanostructures is essential to obtain full compatibility with photonic devices and requires accurate tailoring of structures with predetermined parameters. Therefore it is critical to gain deeper insight into the optical properties of TiO_2/Si nanostructures with different morphology. Due to its fundamental physical properties enhanced by quantum confinement effects, nanostructured TiO_2 in silicon nanocomposites are promising material for designing of novel electro-optical devices [3, 4].

In our previous investigations, we have demonstrated enhanced optical properties of PSi/TiO_2 porous nanostructures which allow us to produce sensitive biosensors capable of detecting various types of molecules [5, 6]. Nevertheless, obtaining and studying of morphology, structure and optical characteristics of such periodic structures, especially with TiO_2 coverage, is still an important issue.

In present work, we have studied structural and optical properties of PSi and silicon nanowires (NW)/nanopillars coated with a TiO_2 layer by Atomic Layer Deposition (ALD) technique. For this purpose, the silicon nanostructures were fabricated using metal-assisted chemical etching (MACE) which had utilized gold and silver thin films as catalysts in the etching process. Optical and structural measurements were carried out. It was shown that these silicon nanocomposites could be used as effective materials for energy storage and solar cells application.

[*]yatsunskiy@gmail.com; phone +47 731308173

Nanophotonics VI, edited by David L. Andrews, Jean-Michel Nunzi, Andreas Ostendorf, Proc. of SPIE Vol. 9884, 98842H · © 2016 SPIE · CCC code: 0277-786X/16/$18 · doi: 10.1117/12.2227122

2. EXPERIMENTAL

Preparation of PSi. The porous silicon (PSi) samples were fabricated from (100) oriented and highly doped p-type Si (B-doped, q < 0.005 Ω×cm) utilizing metal-assisted chemical etching (MACE) [7]. Silicon samples (1 × 1 cm), after standard RCA cleaning, were cleaned with acetone, isopropanol, and deionized water via ultrasonic cleaning. The silver particles, which act as catalysts to assist in the etching of silicon, were deposited on Si samples by immersion in 0.2 M HF and 10^{-3} M $AgNO_3$ metallization aqueous solutions. The time of immersion was 60 s. Then, the samples were etched in aqueous solutions containing HF (40%), H_2O_2 (30%), and ultrapure H_2O at a ratio of 80:80:20 H_2O_2/H_2O/HF for 60 min. After etching, the samples were dipped in HNO_3 solution to remove the silver particles for 30 min and were then dipped in HF (5%) solution to remove an oxide. They were then cleaned with deionized water and blown dry with nitrogen. The etching and immersion procedures were performed at room temperature.

Preparation of the Si nanopillars. Silicon nanopillars were obtained using the same silicon wafer as for previous samples. Polystyrene nanospheres 10% solution of 600 nm was mixed with an equal amount of ethanol and then applied to the deposition of a mask monolayer on a clean silicon surface by floating technique [8]. After deposition the size of spheres was converged to 300 nm using reactive ion etching (RIE) in oxygen plasma. The gold layer, which acts as catalysts to assist in the etching of silicon, was deposited on Si samples by using magnetron sputtering under conditions suitable for layer thickness of 130-140 nm. Then, samples were etched in the same aqueous solutions as for PSi samples for 30, 10 and 5 minutes. After etching, the samples were dipped in solution of aqua regia which comprises HCl (35%) and HNO_3 (65%) at ratio 1:1, to remove the gold layer, and were then dipped in HF (5%) solution for 3 min to remove an oxide. They were then cleaned with deionized water and blown dry with nitrogen. The etching and immersion procedures were performed at room temperature.

ALD Coating. The obtained probes of porous silicon matrix and nanopillars were placed in an ALD reactor (Picosun). The TiO_2 thin films were deposited onto the probes using $TiCl_4$ and water as ALD precursors. Nitrogen (N_2) flow was used as a carrier and purging gas. $TiCl_4$ precursor and water were evaporated at 20 °C. In this study, the standard cycle consisted of 0.1 s $TiCl_4$ exposure, 3s N_2 purge, 0.1s exposure to water, and 4s N_2 purge. The total flow rate of N_2 was 150 standard cubic centimeters per minute (sccm). The TiO_2 thin films were grown at 300 °C. The growth rate was typically 0.5 Å per cycle for TiO_2 on the planar silicon surface. After TiO_2 deposition, some samples were annealed at 400 °C for an hour in an ambient atmosphere.

Material Characterization and Optical Measurements. Structural properties of the obtained PSi, Si nanopillars and PSi/TiO_2 structures were investigated by scanning electron microscopy (SEM) (JEOL, JSM-7001F). Optical properties of the samples have been studied by photoluminescence spectroscopy and reflectance measurements. Photoluminescence (PL) of the samples was measured at room temperatures using a home-made setup which comprise monochromator, photomultiplier tube and support equipment. The excitation of PL was performed with a nitrogen laser (337.7 nm), and the emission spectra were recorded in the range of 400−850 nm. Reflectance measurements were performed by UV-VIS-IR PerkinElmer spectrophotometer Lambda 950.

3. RESULTS AND DISCUSSIONS

Morphology peculiarities of PSi and PSi/TiO_2 samples. Fig. 1 shows SEM images of PSi and PSi/TiO_2 structures. Fig.1a depicts porous silicon surface obtained by MACE method. It is clearly seen the macro porous having pyramid-shaped. The average pore size is in the range of 1.5-2 μm. Inner wall of the macropores had mesoporous structure with an average diameter of pores about 10 nm (Fig.1b). It might be suggested that during ALD processes not only macroporous structure will be covered by TiO_2 but mesopores as well. Peculiarities of this complex porous structure (macro and meso-PSi) can be explained by typical model of MACE proposed by Chartier et al [9]. According to this model, the etching process occurs at pore walls and pore tips with different rate due to difference in holes injection flux, which prevails at the pore tips on interface between noble metal particles and silicon. Thus, widening and dipping of pores occurs with different rates, which also depends on crystal orientation, doping concentration and type of silicon. Taking into account, that the formation of the macropore occurs in the localization of noble metal particle, the diffusion of holes along the macropore wall leads to the generation of mesoporous layer. Detailed characterization of this mechanism was discussed in our previous paper [10].

Typical plan-view SEM images of PSi coated with TiO_2 are shown in Fig. 1 c, d. Fig. 1 c shows the PSi matrix covered with TiO_2 layer. This layer was formed under 200 ALD cycles which corresponds to approximately 10 nm thickness for the plain surface. It is clearly seen, that the PSi surface is conformally covered by TiO_2. The TiO_2 layer had granular structure. The average diameter of TiO_2 nanograins was about 8-10 nm.

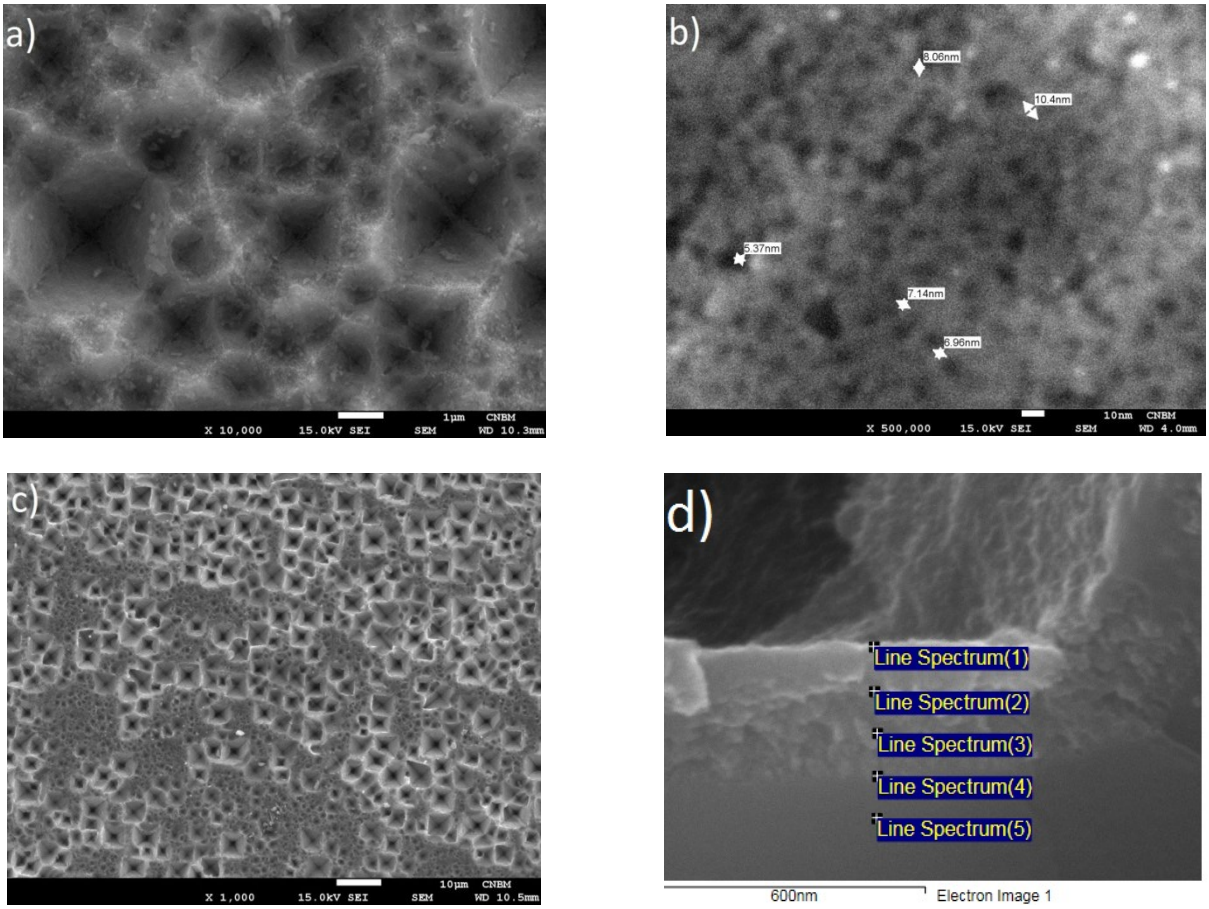

Fig.1.SEM images of: a) PSi surface obtained by MACE; b) high resolution image of mesoporous silicon surface, size of pores is in range of 5 to 10 nm; c) initial PSi surface on fig.1a covered by 200 ALD cycles of TiO_2; d) the cross-section SEM image of a meso pore.

Table 1. Atomic percent concentration of elements in cross-section on Fig. 1d.

Line Spectrum	C	O	Si	Ti
1	4,62	44,35	40,12	10,90
2	7,26	45,64	36,15	10,94
3	8,29	41,86	38,98	10,87
4	9,23	27,36	56,59	6,82
5	9,78	21,08	64,15	4,99

Fig. 1d demonstrates a cross-section view of TiO_2 layer of meso-PSi layer. Five point EDX measurements were performed on a meso-PSi layer, as indicated in Fig. 1d. Cross-sectional SEM image indicates that TiO_2 infiltrates and conformally coats the meso-PSi. In order to characterize the chemical composition of meso-PSi layer, EDX measurements were carried out. Table 1 shows the distribution of titanium, oxygen atoms and other elements presented inside the meso-PSi. Atoms of titanium penetrate inside the mesoporous Si layer. Atomic ratio of Ti atoms in the meso-PSi layer has a permanent trend up to the interface between the Si and PSi. Beyond the interface a concentration of Ti atoms sharply decrease. The concentration of oxygen atoms inside the meso-PSi layer is approximately 43% and the concentration ration of O/Ti~4. Taking into account, that stoichiometry (ration O/Ti) of crystalline TiO_2 is equal to 2. The excess of oxygen atoms could be consumed for Si oxidation.

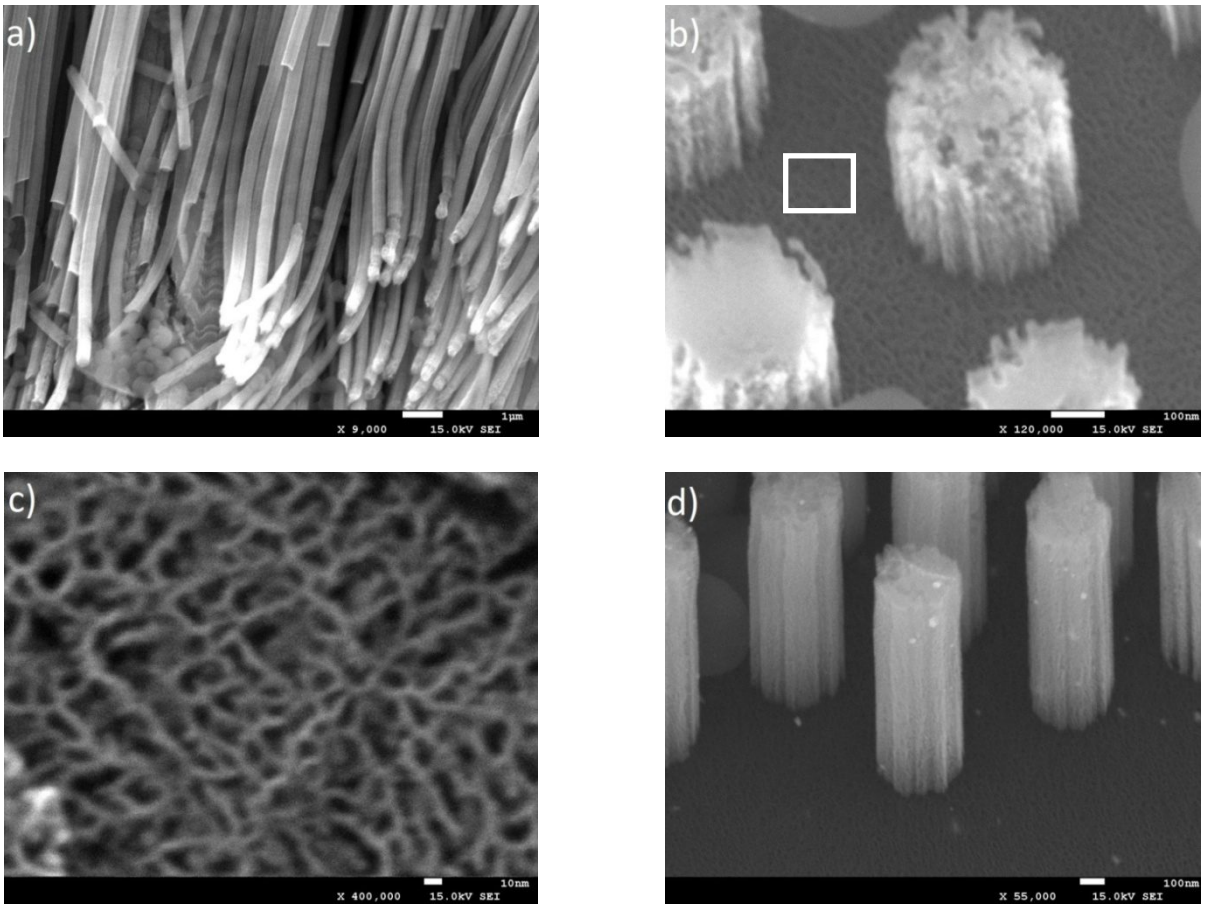

Fig.2. SEM images of silicon nanopillars obtained under a) 30 min etching; b) 5 min etching; c) mesoporous surface in pillar vicinity of high doped p-type silicon under high resolution (white square in Fig,2b); d) 10 min etching

Morphology of TiO_2 coated nanopillars samples. Fig. 2a depicts a disordered NW array obtained within 30 min etching. NWs have a diameter of 200 nm and a substantial length more than 10 µm. The average distance between two pillars is 400 nm. Significant etching time (about 60 minutes) leads to deformation and convolving of Si NW under mechanical stresses. Some of the NWs are torn off from the substrate. Decreasing the etching time (5-10 min) leads to the forming of stable NW arrays without considerable influence of mechanical stresses (Fig.2b, d). These arrays hold an ordered hexagonal structure which attributed to the order of deposited monolayer polystyrene mask. Structural

peculiarities of this ordered NWs resemble a pillar structure with straight grooves and convexes at its wall (Fig. 1b). For high doping p-type silicon, we obtained nanopillars having mesoporous structure (Fig. 2b). The mesoporous structure was also formed on the silicon surface due to high catalytic etching of bulk silicon under the gold layer (Fig. 1c). Average size of mesopores is approximately 10 nm.

After 200 ALD cycles, approximately 10 nm layer of TiO_2 was coated on the surface of the silicon nanopillars. The TiO_2 layer had also the granular structure. The individual size of grains was around 10nm. The inside of the porous Si nanopillars was also partially filled by TiO_2. For both nanomaterials, a PSi and silicon nanopillars, the titanium oxide was in an amorphous phase (XRD results are not shown in this work).

Optical properties. In the final stage of our research, some optical studies were performed. Figure 3a shows PL spectra of PSi and PSi covered by TiO_2. PSi depicts the main PL peak in a visible spectral range at 1.8 eV (about 690 nm). Samples of PSi/TiO_2 structures have showed two broad peaks at 2.4-3 eV and 1.7-1.9 eV which correspond to blue and red components, respectively (Fig.3 a). In order to obtain information on the PL mechanisms, we performed Gaussian multipeak fitting. Seven PL bands were obtained after fitting (Fig.3 b). PL band at 2.95 eV corresponds to the self-trapped exciton states localized on the TiO_6 octahedral [11]. The PL bands at 2.74 and 2.48 eV are attributed to oxygen vacancies with two and one electrons respectively. The PL bands at 2.61 eV originates from neutral oxygen vacancy or surface Ti-OH states. The band at 2.2 eV corresponds to the trap lavel related to oxygen vacancies on the surface. The peaks at 1.93 and 1.63 eV related to the surface states change their location and intensity due to redistribution and decreasing of the surface state amount after annealing.

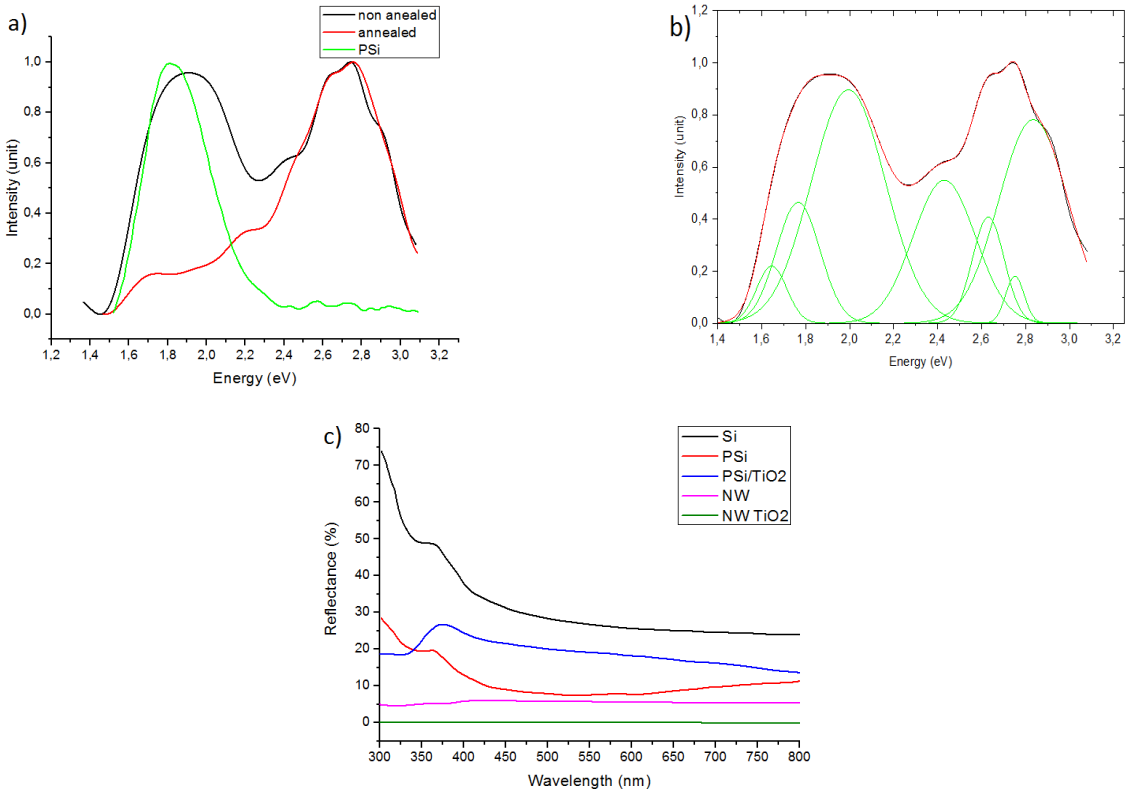

Fig.3. Photoluminescence of PSi/TiO_2 nanostructures: a) with 200 ALD cycles before (black curve) and after (red curve) annealing; b) PL spectrum before annealing fitted with elementary Gaussian peaks; c) total reflectance spectra of Si nanostructures.

Fig. 3c shows the reflectance spectra of PSi and silicon nanopillars. The reflection spectrum of a Si substrate is also presented for the purpose of comparison. The reflectance of the Si (black curve) is about 35 % as expected while the reflectance is significantly decreased after the formation of PSi (red curve) and silicon nanopillars (magenta curve) with an average value of about 10 % and 6 %, respectively. The low reflectance can be attributed to the strong light trapping ability of the silicon nanostructures.

A resonant reflection can be observed at 350-400 nm for PSi/TiO_2 reflectance spectrum (blue curve). The reflectance of PSi/TiO_2 is larger (20%) than for the PSi sample. It could be explained by influence of TiO_2 layer which constrains the diffusion scattering at porous surface.
The lowest reflectance (less than 2-3 %) was indicated for silicon nanopillars covered by TiO_2 (magenta curve in Fig. 3 c). It is clearly seen that silicon nanopillars covered by TiO_2 acted as antireflection coating. The incident light on silicon nanopillars coated by TiO_2 suffered more scattering and hence the absorption. In case of TiO_2 coated Si nanopillars, the UV photons were absorbed by the TiO_2 and UV-visible region by Si.

4. CONCLUSION

In present paper, we have studied the structural and optical properties of PSi nanostructures and silicon nanopillars fabricated by ALD and MACE techniques by means of electron microscopy, energy dispersive X-ray, photoluminescence and reflectance spectroscopy. Main structural and optical characteristics were discussed. Peculiarities of PSi/TiO_2 morphology defined and explained in frames fabrication technology. It was shown, that the observed low reflectance effect in silicon nanocomposites could be applied in solar cell technology as antireflectance coating. The TiO_2 coverage decreases reflective properties especially at UV region.

REFERENCES

[1] Mohammadreza, K., Simarjeet, S., "Silicon nanowire optical waveguide (SHOW)," OSA Publishing, Optics Express, vol.18 (22), 23442-23457, (2010).

[2] Nduwimana, A., Xiao-Qian, W., "Tunable electronic properties of silicon nanowires under strain and electric bias," AIP Advances, vol. 4, 077122, (2014).

[3] Seo, D., Lee, J.," Structural modulation of silicon nanowires by combining a high gas flow rate with metal catalysts," PubMed, vol.10, 190, (2015).

[4] Kui-Qing, P., Xin W., "Silicon nanowires for advanced energy conversation and storage," Nanotoday, vol.8 (1), 75-97, (2013).

[5] Iatunskyi, I., Pavlenko, M., Viter, R., et al., "Tailoring the Structural, Optical, and Photoluminescence Properties of Porous Silicon/TiO_2 Nanostructures," J. Phys. Chem. C, vol. 119, 7164−7171, (2015).

[6] Iatunskyi, I., Jancelewicz, M., Nowaczyk, G., et al., "Atomic Layer Deposition TiO_2 Coated Porous Silicon Surface: Structural Characterization and Morphological Features," Thin Solid Films, vol. 589, 303-308, (2015).

[7] Han, H., Huang Z., Lee W., "Metal-assisted chemical etching of silicon and nanotechnology applications," Nanotoday, vol.9 (3), 271-304, (2014).

[8] Biswas, A., Bayer, I., et al., "Advances in top–down and bottom–up surface nanofabrication: techniques, applications & future prospects," Advances in colloid and interface science, vol. 170, 2–27, (2012).

[9] Chartier, C., Bastide, S., Levy-Clément, C., "Metal-Assisted Chemical Etching of Silicon in HF−H_2O_2," Electrochim. Acta, vol.53, 5509-5516, (2008).

[10] Iatsunskyi, I., Kempiński, M.; Nowaczyk, G., et al., "Structural and XPS studies of PSi/TiO_2 nanocomposites prepared by ALD and Ag-assisted chemical etching," Applied Surface Science, vol. 347, 777–783, (2015).

[11] Choudhury, B., Choudhury, A., "Tailoring Luminescence Properties of TiO_2 Nanoparticles by Mn Doping," J. Lumin, vol. 136, 339−346, (2013).